Proceedings World Geothermal Congress 2010
Bali, Indonesia, 25-29 April 2010

An Inverse Approach for Estimation of Initial Formation Temperatures

Alfonso García-Gutiérrez[1,2], Ulises Olea-González[2,3] and Jose R. Ramos-Alcántara[2]

[1] Instituto de Investigaciones Eléctricas, Ave. Reforma 113, Palmira, Cuernavaca, Mor., 62490 México

[2]Centro Nacional de Investigación y Desarrollo Tecnológico, Av. Palmira s/n, Cuernavaca, Mor., 62490, México

[3] Instituto Mexicano del Petróleo, Dirección de Exploración y Producción, Cd. del Carmen Campeche, México

aggarcia@iie.org.mx; uolea@imp.mx; jose.ramos@mex.bellota.com

Keywords: Formation temperature, numerical simulation, inverse problem, proportional control, proportional-integral control

ABSTRACT

An inverse method for the estimation of geothermal and oil reservoir initial formation temperatures IFTs is presented. It is based on control theory whereby temperatures in the well are computed starting from an assumed reservoir temperature profile and compared with logged temperatures at different shut-in times. The comparison is performed using a control algorithm which changes the assumed reservoir temperature profile until the best fit is attained. Fluid and heat flow in the well include circulation and shut-in in the presence of lost circulation transport processes in the formation consider the reservoir as a porous medium. The first part of the algorithm included proportional control (PC) and was applied to well LV-3 from the Las Tres Virgenes Mexico, geothermal field whereby the estimated IFTs compared with measured IFT within ± 15ºC, an acceptable result from an engineering point of view. In the second part, the algorithm was extended to include proportional and integral control PIC. Results of application from an oil well also show that it is feasible to predict IFTs reasonably by this method. IFTs obtained with the latter method also compare well with simpler methods like the Horner and spherical-radial flow method.

1. INTRODUCTION

Knowledge of the formation temperature is important in many areas of engineering and scientific research related to the development and exploitation of geothermal and oil reservoirs, such as reservoir engineering, well completion, production logging, estimation of reserves, evaluation of energy and fluid reserves, and of formation thermal properties, among others. This information is also considered as a vital tool for a correct design of the drilling fluid and cement slurry programs and for deciding whether drilling should be stopped or continued (e.g., Grant et al., 1969; Ascencio et al., 1994; Takahashi et al., 1997; Garcia et al., 2000). IFTs in wellbores can be inferred from temperature logging (Dowdle and Cobb, 1975; Ascencio et al., 1994); empirical correlations (Farris, 1941; Kutasov and Targhi, 1987), analysis of fluid inclusions (Fujino and Yamasaki, 1985) or by numerical simulation whereby logged temperatures during well drilling are reproduced (Luhesi, 1983; Garcia et al., 2000; Takahashi et al., 1997; Osato et al., 2003). Numerical simulation is a complex task and usually requires a great deal of information on drilling fluid composition, inlet fluid temperatures, fluid circulation rate and circulation losses, well geometry characteristics, geothermal gradient (a guess on the initial condition which is used to start the simulation, and is a related to the IFT), and thermophysical properties.

Drilling of a wellbore is essentially a transient process due to circulation (cooling) and shut-in (heating) processes. During well drilling, the formation temperature is perturbed from the original condition (IFT), which in practice is unknown. Thus, inverse heat transfer problems used to determine IFTs are based on directly measured quantities such as bottom-hole temperatures (BHT) or temperature logs. This is a typical inverse problem, in contrast to the direct problem, whereby the temperature field (BHT) is computed from the initial condition (IFT), that is, the inverse problem is associated with the reversal of the cause-effect sequence and consists of finding the unknown causes (IFT) of known consequences (BHT). The solution of an inverse problem is not straightforward and requires numerical techniques to stabilize the results of calculations. A commonly used algorithm for solving inverse problems is based on non-linear least squares and is known as the Levenberg-Marquardt algorithm (Marquardt 1963). More recently (Ramos-Alcantara, 2004; Olea-Gonzalez, 2007; Olea-Gonzalez and García-Gutiérrez, 2008; García-Gutiérrez et al., 2009) included Proportional Control PC and Proportional-Integral control PIC algorithms in inverse formulations to estimate IFTs.

This paper deals with the estimation of IFTs based on the inverse solution of a 2D fully-transient heat transfer problem in a well with convective and conductive mechanisms using BHT measurements. Two algorithms, one based on proportional control PC and another based on proportional integral control PIC are used to solve the inverse problem whereby computed BHT temperatures are compared with logged temperatures at different shut-in times and depths.

2. INITIAL FORMATION TEMPERATURES

2.1 Solution Outline

Numerical simulation of the circulation and shut-in processes were used to compute the temperature field in the well and surrounding formation. Drilling mud shut-in temperatures were then fitted to logged temperatures at different times and depths using the inverse control algorithms described below. The simulation of the circulation and shut-in processes starts from an assumed IFT profile and data on the well and circulation losses taken from well drilling records. Computed mud shut-in temperatures are then fitted to logged temperatures at different times and depths using the PC and PIC control algorithms. If the comparison is not satisfactory, the respective control algorithm varies the IFT until an error criterion is satisfied. The last version of the formation temperature profile is taken as the IFT.

2.2 Proportional Control PC Algorithm

In this case, the IFT is computed using the PC algorithm (Ramos-Alcantara, 2004) which provides a control action on the regulation error:

$$\frac{dT_{ift}}{dt} = -\frac{e_{reg}}{\tau} \quad (1)$$

where τ is a time constant and e_{reg} is a regulation error. At the set point, the regulation error is defined as $e_{reg} = (T_{log} - T_{sim})$. Substitution of this expression and using a finite difference approximation for the derivative in Eq. (1) it follows that:

$$T_{ift}^{t+\Delta t} = T_{ift}^{t} - \frac{(T_{\log} - T_{sim})}{\tau^*}; \quad \tau^* = \frac{\tau}{\Delta t} \quad (2)$$

where t+Δt indicates present time and t denotes past time. The basic idea is contained in Fig. 1 which indicates that logged temperatures are available as well as temperatures simulated at nearly the same conditions of the measured data. These two sets of temperatures are compared point by point until both sets fit with each other. This process depends on a number of independent variables, but mainly on the initial formation temperature, i.e., the initial condition of the mathematical problem. The control algorithm changes the fitting variable automatically.

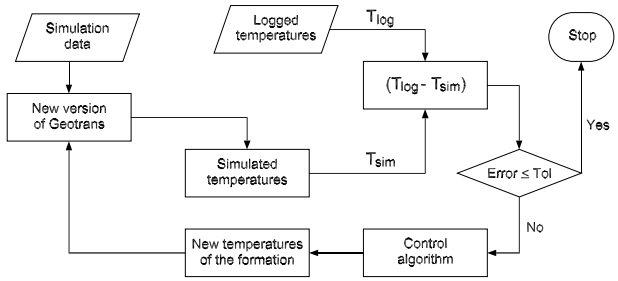

Figure 1: The inverse problem PC algorithm.

2.3 Proportional Integral Control PIC Algorithm

The idea of the method is that the axial profile of the *simulated* logged-temperature tracks the axial profile of the *measured* logged temperatures (BHT) using the PI control approach. From the point of view of control theory the logged temperatures represent the set point. The PI control is used to estimate the SFT from logged (Tlog) and simulated (Tsim) temperatures. The PI control in Laplace transform is given by:

$$\mathrm{PI} = K_p e(s)\left[1 + \frac{1}{\tau_1 s}\right] \quad (3)$$

where K_P and τ_1 correspond to the proportional gain and integral time, respectively, and represent the PI control adjusting parameters. The tracking instantaneous error is given by:

$$e(s) = (T_{\log} - T_{sim}) \quad (4)$$

which is defined as the difference between the logged and simulated temperatures Applying discrete PI control, then the iteration process with PI action can be represented by:

$$T_{SFT}(k+1) = T_{SFT}(k) + K_p\left[e(k) + I(k+1)\right] \quad (5)$$

$$e(k) = T_{\log}(k) - T_{sim}(k) \quad (6)$$

$$I(k+1) = \frac{1}{\tau_I}\int_0^k e(s)ds + \frac{\Delta t}{\tau_I}e(k) \quad (7)$$

Here T_{SFT} $(k+1)$ represents a new SFT value at k+1, and Δt is the time step. These equations are applied for all the spatial grid points at the (k+1)th iteration. Fig. 2 illustrates the PI method.

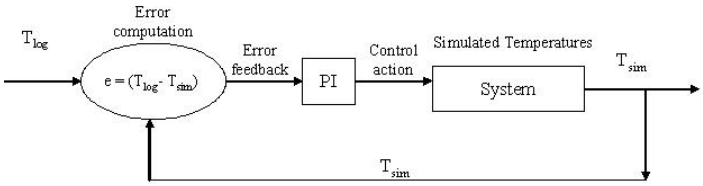

Figure 2: Block diagram of feedback control in the PIC algorithm.

3. MATHEMATICAL MODEL

3.1 Heat Transfer in the Well

The well thermal model has been described in detail elsewhere (García-Gutierrez et. al., 2000) and only a summary is given here. The simulated temperature $T_{sim,,}$ Eqs. (2) and (4), is obtained from the well model and is represented by the computed annulus temperature. Fig. 3 shows the process of drilling fluid circulation which is similar to a heat exchanger. Drilling fluid flows downwards inside the drill pipe and upwards in the annulus. Thus, the system acts a counterflow heat exchanger with additional exchange with the surrounding formation If lost circulation exists, some fluid flows to the formation. The thermal problem consists of a set of heat transfer partial differential equations describing the 2D transient temperature field T(z,r,t). Mass conservation considers incompressible flow in the axial and radial directions. The solution also considers the heat transfer convective effects. The well-formation interface is considered as a porous medium through which fluid may be lost or gained by the well. The mathematical formulation is generic since any vertical well can be studied and fluid loss or gain can be simulated at any point in the well. During shut-in, heat conduction dominates the return to thermal equilibrium.

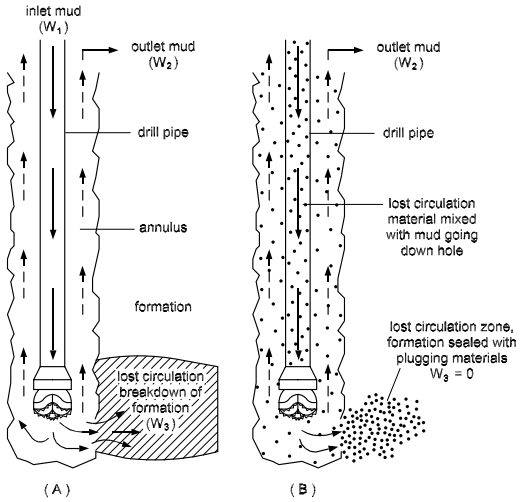

Figure 3: Physical model of drilling fluid circulation and circulation losses during well drilling.

The fundamental assumptions are:

(1) Axis-symmetric heat
(2) Isotropic rock formation with homogeneous porosity
(3) Formation, cement, pipe metal and drilling fluid constant properties
(4) Negligible viscous dissipation effects
(5) No natural convection exists after shut-in

With these considerations, the energy and continuity equations reduce to:

$$\rho C_p\left(\frac{\partial T}{\partial t}+v_r\frac{\partial T}{\partial r}+v_z\frac{\partial T}{\partial z}\right)=k\left(\frac{1}{r}\frac{\partial T}{\partial t}+\frac{\partial^2 T}{\partial r^2}+\frac{\partial^2 T}{\partial z^2}\right) \quad (8)$$

$$\frac{1}{r}\frac{\partial\left(r\,v_r\right)}{\partial r}+\frac{\partial v_z}{\partial z}=0 \quad (9)$$

where *r*,z are radial and axial coordinates, T is temperature, v is velocity, ρ is density, Cp is specific heat and k is thermal conductivity. The initial and boundary conditions are:

I. C.: $T(r, z, t=0) = f(r, z) =$ unknown (10)

BC1: $$-k\left(\frac{\partial T}{\partial r}\right)_i = h\left(T_s - T_f\right) \text{ on } A_i \text{ for all } t \quad (11)$$

BC2: $$\left(\frac{\partial T}{\partial r}\right)_{r=0} = 0 \text{ at } r=0 \text{ for all } t \quad (12)$$

BC3: $$T(r,z,t)=T_0;\ z=0;\ t>0 \quad (13)$$

BC4: $$T(r,z,t)=T_D;\ z=D;\ t>0 \quad (14)$$

BC5: $$v_z = W/\rho A_f \text{ at } z=0 \text{ for all } t \quad (15)$$

BC6: $$v_r = f\left(\phi, W_{loss}, \rho, A_l\right) \text{ on } A_i \text{ for all } t \quad (16)$$

where T_s is the solid temperature, T_f is the fluid temperature, T_0 is the temperature at the surface, T_B is the temperature at maximum depth, r and z are the radial and axial coordinates, A_i is the interfacial area between the rock formation and the fluid, W is the drilling fluid inlet mass flowrate, D is total depth, A_f is the cross sectional area for flow, ϕ is the formation porosity and A_l is the lateral flow area. Equations (8)-(16) define in generic form the problem posed and their application follows a simplified scheme of the physical drilling system where the various regions for heat flow are defined. Fig. 4 shows schematically an axial region of length Δz, and the location and spacing of the radial mesh. The radii of this figure correspond to each one of the physical regions in which the well is divided. Five regions or components were identified as necessary in the heat transfer analysis: (1) the drill pipe; (2) the drill pipe wall; (3) the annular region; (4) the interface between the well wall (cement or rock formation) and the annular region for fluid return; and (5) the surrounding formation. Based on this configuration, a numerical method and a computer code were developed by consideration of a complete mathematical formulation of each of these regions defined in Fig. 4.

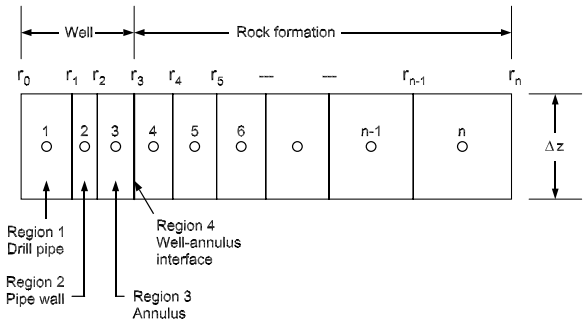

Figure 4: Well and formation radial node distribution. The radius r indicates the boundaries of each radial region or cell and "o" indicates the cell where the computations are performed.

Eqs. (8) to (16) are specialized to estimate temperatures in regions 1-4, as in the original model, however, in the present study formation temperatures are obtained from a single-equation volume-averaged model derived from the individual equations of the solid and fluid phases while considering the formation as an isotropic porous medium, where 2D heat conduction and convection are accounted for. The modified version of the simulator also includes models on the hydrodynamics of the well and surrounding formation to estimate the pressure and velocity fields.

3.2 Heat Transfer in the Formation

The volume-averaged model used in this work is based on mass, energy and momentum balances which consider flow in a porous medium as flow in an effective medium (Ramos-Alcantara, 2004; Garcia-Gutierrez et al, 2009). Since the flow is located in the interstices or pores of the reservoir, the transient energy equation considers 2D heat transfer by conduction and convection. The geothermal reservoir is considered as a fractured porous medium as illustrated in Fig. 5, where the σ-phase represents a rigid, impermeable solid phase and the o-phase represents an incompressible fluid. The averaging volume chosen is used to develop the volume-averaged model of mass, momentum and energy transport.

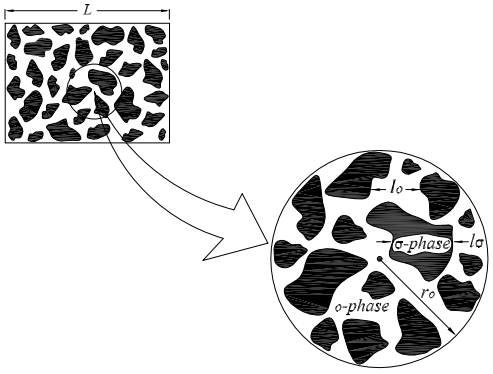

Figure 5: Averaging two-phase volume of a geothermal reservoir.

The volume-averaged model of energy transport in a geothermal system is obtained as a single-equation model from the averaged transport equations of the individual solid and fluid phases and the use of the principle of local thermal equilibrium.

$$\langle\rho\rangle Cp\frac{\partial\langle T\rangle}{\partial t}+(\rho Cp)_o\langle\mathbf{v}_o\rangle\cdot\nabla\langle T\rangle=\nabla\cdot\left[\mathbf{K}^*\cdot\nabla\langle T\rangle\right] \quad (17)$$

I. C.: $\langle T\rangle(r, z, t=0) = f(r, z)=$ unknown (18)

BC1A: $$-k_{eff}\left(\frac{\partial\langle T\rangle}{\partial r}\right)=h\left(T_s-\langle T\rangle\right)_{r_3} \quad (19)$$

BC1B: $$\langle T\rangle(r,z,t) = T_3(r_3,z,t) \quad (20)$$

BC2: $$\langle T\rangle (r,z,t)=f(z),\ r\rightarrow\infty\ ;t>0 \quad (21)$$

BC3: $$\langle T\rangle (r,z,t)=T_0;\ r>r_3,\ z=0,\ t>0 \quad (22)$$

BC4: $$\langle T\rangle(r,z,t)=T_D;\ r>r_3,\ z=D,\ t>0 \quad (23)$$

In Eq. (15), $\langle \mathbf{V}_O \rangle$ is the superficial average velocity, $\langle T\rangle$ is the spatial average temperature, $\langle\rho\rangle Cp$ is the product of the average density and the heat capacity of the effective medium, $(\rho Cp)_o$ is the product of the density and the heat capacity of the fluid phase and $\mathbf{K}^*(=\mathbf{K}_{eff}+\mathbf{K}_D)$ is the total effective thermal conductivity tensor which includes the contribution due to thermal dispersion. Boundary conditions BC1A and BC1B define, respectively, a convective boundary due to circulation losses and a constant temperature boundary for the rest of the well. Once the velocities are known, Eq. (17) can be used to determine the spatial average temperatures. The solution of this problem is described elsewhere (Ramos-Alcantara, 2004; Garcia-Gutierrez et al, 2009).

3.3 Hydrodynamic Model of the Well

Macroscopic momentum balances were derived to compute the axial pressure and velocity profiles of the fluid in the drill pipe and annulus assuming fully developed steady-state flow, incompressible drilling fluid with constant thermal and transport properties, and constant flow area along the axial direction. In terms of mass, the resulting equations are:

$$\frac{1}{A}\frac{\partial W}{\partial z}-\phi=0 \quad (24)$$

$$\frac{1}{A^2}\frac{\partial W^2}{\partial z}=-\frac{\partial p}{\partial z}-\frac{fW^2}{2A\rho}-\rho g \quad (25)$$

where W is mass flow rate, f is the friction coefficient, A is cross sectional area, p is pressure,ρ is density, g is the acceleration due to gravity and ϕ is a source term which represents fluid losses to the formation, and is zero in the drill pipe. Mass balance in the annulus is given by:

$$W_1 = W_2 + W_3 \quad (26)$$

where W_1 and W_2 are the inlet and outlet mass flow rates and W_3 is the mass flow that is lost to the formation.

3.3 Hydrodynamic Model of the Formation

The hydrodynamic model of the formation is a one-dimensional volume-averaging model that governs the flow of an incompressible fluid through an isotropic porous medium given by:

$$\langle u_r\rangle=-\frac{K}{\mu}\frac{\partial\langle p\rangle}{\partial r} \quad (27)$$

$$\frac{K}{\mu}\frac{\partial^2\langle p\rangle}{\partial r^2}+\frac{1}{r}\frac{K}{\mu}\frac{\partial\langle p\rangle}{\partial r}+\frac{q}{\rho}=0 \quad (28)$$

BC1: $$\begin{cases}\dfrac{\partial\langle p\rangle}{\partial r}=0;\ impermeable\quad wall\\ \langle p\rangle=p\big|_{r_3};\ permeable\quad walll\end{cases} \quad (29)$$

BC2: $$\frac{\partial\langle p\rangle}{\partial r}=0;\ r\rightarrow\infty \quad (30)$$

In these equations, u_r *is* radial velocity, p is intrinsic pressure, q is a source term, and K is the absolute permeability of the porous medium which is computed form the Blake-Kozeny model (Whitaker, 1999). Boundary conditions BC1 and BC2 are the fluid flow equivalent of boundary conditions BC1A and BC1B of the the heat transfer formation model.

The initial condition given by Eq. (10) represents the IFT which is unknown. The input data required by the feedback control algorithms to minimize the error during the fitting process are the simulated and the experimentally measured or logged temperatures during shut-in which represents a particular solution of Eq. (8). In other words, the profile of the simulated *logged-temperatures* tracks the profile actually logged temperatures using the PC and PIC algorithms. In control theory, the logged temperatures are equivalent to the set point of the system.

The equations described above were solved using finite differences in order to obtain the temperatures in the well and formation during circulation and shut-in in presence of circulation losses by numerical simulation. The resulting annulus temperatures at different times and depths during shut-in were fed to the control algorithms to perform the temperature inversion and to determine the IFTs.

4. RESULTS AND DISCUSSION

4.1 Application of the PC algorithm

The PC algorithm was applied to the estimation of the IFTs of well LV-3 from the Las Tres Virgenes, Mexico, geothermal field. The well had circulation between 1281m and 1671 m. Shut-in temperatures were logged at shut-in times between 6 and 24 hours down to the 1996 m depth. The data used for this case is given in Table 1 while logged temperatures in well LV-3 at 6, 12, 18 and 24 hours shut-in are shown in Fig. 6 (Garcia-Gutierrez et al, 2009).

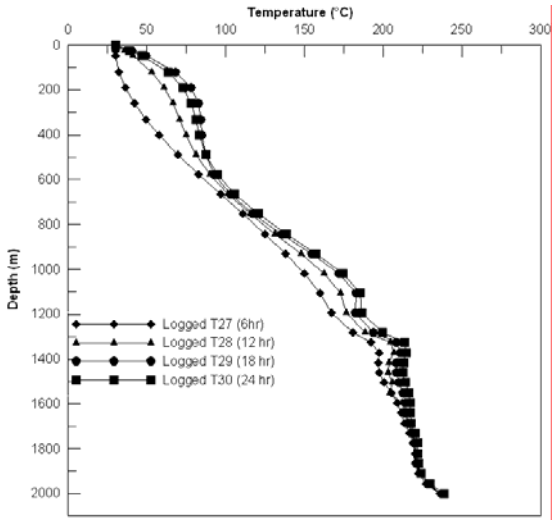

Figure 6: Well LV-3 logged temperatures

Table 1: Data of well LV-3.

Well Geometry				
Drilling stage	**1**	**2**	**3**	**4**
Diameter, m	0.66	0.44	0.31	0.22
Length, m	48.00	354.00	879.00	719.00
DP diameter, m	0.1143	0.1143	0.1143	0.1143
Wall thickness, m	0.0074	0.0074	0.0074	0.0074
Thermal and transport properties				
Material	**K W/(m^2-K)**	**Cp J/(kg-K)**	**ρ kg/m^3**	**μ Pa-s**
Formation	1.90	940.00	2600	
Cement	0.70	2000.00	3150	
Metal	43.0	440.00	7800	
Drilling fluid	0.24	2000.00	280	0.000076
Temperature and flow data				
Inlet temperature °C	**Surface temperature °C**	**Mass flow rate kg/s**	**Geothermal gradient °C/m**	
30.00	30.00	24.72	0.12	

Using the mathematical model and the control-based inverse algorithm described above, the simulated well temperatures were obtained and fitted to the logged temperatures. Fig. 7 shows a comparison of the simulated and logged temperatures at different shut-in times as well as the simulated and field-measured IFTs. From the figure, it is observed that the simulated shut-in temperature profiles match satisfactorily the logged temperatures. The largest temperature difference (14°C) occurred between 1000 and 1200 m depth at a shut-in time of 6 hours, however the matching between logged and simulated temperatures improves at greater shut-in times at all depths. In the depth range where the greater discrepancies were found the thermal recovery rate observed from the measured data seems to be slower than that from the simulated results for early shut-in times. This may be due to the actual effect that temperature has on the thermophysical and transport properties of the well materials and drilling fluid, however in the present study they are assumed as constant since no sufficient data is available to account for this effect.

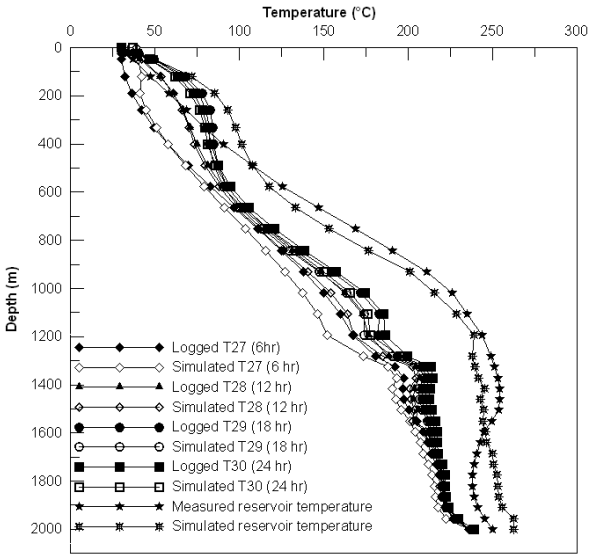

Figure 7: Simulated and logged temperatures of well LV-3. Also shown are the simulated and measured reservoir initial temperature profiles.

Further analysis of Fig. 7 shows that the 6-hour shut-in temperature log differs qualitatively from the temperature logs measured at greater shut-in times in the depth intervals from 0 to 600 m and from about 900 to 1200 m. However, these depth ranges are above the permeable horizon (1300 – 2000 m) and hence this finding may be marginal from a point of view of geothermal fluid production. Conversely, a satisfactory agreement between logged and simulated temperatures was obtained in the depth range where circulation losses occurred (1281-1685 m).

From Fig. 7, it is also observed that the field-measured and simulated IFTs are in good concordance. The typical difference is about 7% (≈13°C) from 500 m to total well depth however between 100 m and 400 m the differences are higher, with a maximum of about 26% (≈19.8°C) at 331 m. These higher differences are far from the productive reservoir zone and are acceptable from an engineering point of view.

Fig. 8 shows a simplified version of Fig. 7. In this case, only the simulated and logged temperatures at 24 hours shut-in time are shown as well as the simulated and measured initial formation temperatures. From this figure, the satisfactory match between the logged and simulated temperature profiles and the concordance between the field-measured and simulated initial reservoir temperature profiles is clearly seen. These findings indicate that the present methodology is adequate for estimating the initial formation temperature from well drilling data and that the mathematical model provides a good approximation of the circulation and shut-in periods in the well. The inversion algorithm also properly matches the logged and measured temperatures while changing IFT, i.e., the unknown initial condition of the inverse problem, until the best match is found and the resulting formation temperatures compare satisfactorily with measured data. It is worth mentioning that modeling in sufficient detail the zone of the reservoir with circulation losses leads to a better estimation of the unperturbed reservoir temperatures and further modeling efforts should improve these estimations.

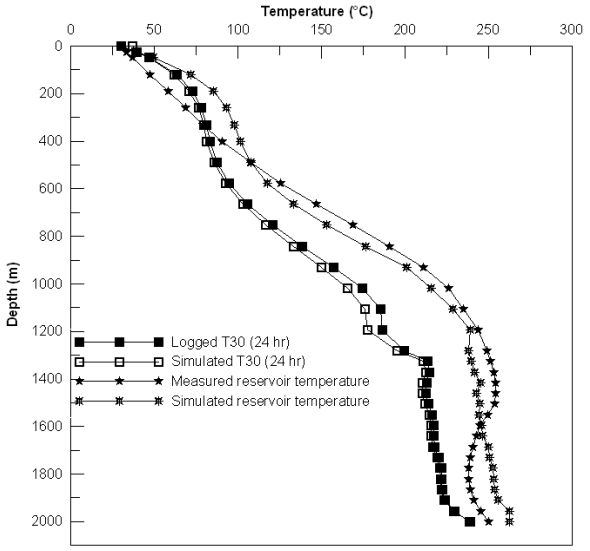

Figure 8: Simulated and logged temperatures at 24 hour shut-in time of well LV-3. Also shown are the measured and simulated reservoir initial temperature profiles.

4.2 Application of the PIC algorithm

The estimation of SFT using the PIC inverse algorithm was done using field data of oil well A. The well data is given in Table 1. The true reported IFTs for this well include a linear

geothermal gradient of 3°C/100 m between 25°C at zero depth and 110°C at a depth of 3500 m (Olea-Gonzalez and Garcia-Gutierrez, 2008).

Figure 9 shows IFTs obtained by the PIC algorithm. Also included are IFT estimations using simpler methods like the Horner method, the spherical-radial heat flow method of Ascencio et al. (1994); the Hassan et al. (1991), and the Kritikos and Kutasov (1988) method. As mentioned before the reported true IFT for this well is a linear gradient between 25°C at the wellhead and 110°C at 3500 m depth. From the figure it is observed that all methods, inverse and simpler analytical ones, follow a linear trend all the way from the wellhead to the bottom of the well. The exceptions to this behavior are described next. (1) At about 2200 m, the Kritikos and Kutasov (1988) method shows the highest temperature of all methods and this fact appears to be related to the abrupt change in heat conductance of the well in changing from a cemented stage to the deeper uncovered part of the well. (2) At the well bottom, the temperatures predicted by the simpler analytical methods are in reversed order from that observed at 2200 m depth. At this depth, the IFTs predicted by the PIC algorithm are somewhat higher than the IFTs predicted by the analytical methods.

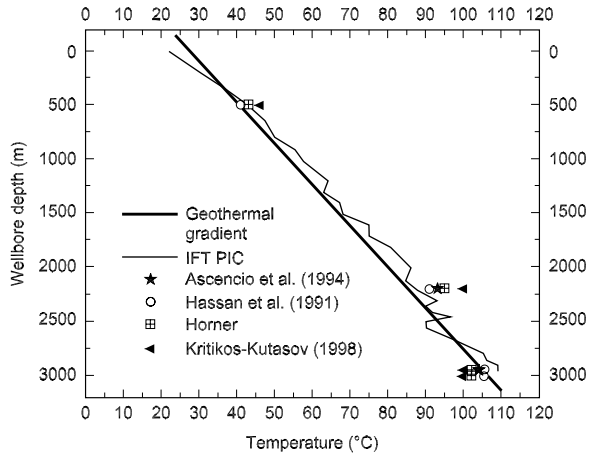

Figure 9: Comparison of IFTs estimated by the PIC inverse control algorithm and other commonly use simper methods.

5. CONCLUSIONS

A methodology based on PC and PIC feedback control was implemented to solve the inverse heat transfer problem for estimation of initial formation temperatures, IFTs from logged and simulated temperatures in a wellbore during shut-in. The temperature behavior in the wellbore has been successfully modeled according with our results. The performance of the method is illustrated by means of the simulation of a geothermal and an oil well. In the latter case, simpler methods like the Horner (Dowdle and Cobb, 1975, the spherical-radial heat flow (Ascencio et al, 1994), the Hasan and Kabir (1994) and Kritikos-Kutasov (1988) were also used for comparison purposes.

For the geothermal well LV-3, comparison of measured and computed unperturbed formation temperatures showed a typical difference of 7% (≈13°C) from 500 m to total depth with a maximum of about 26% (≈19.8°C) at 331 m. These results are acceptable from an engineering point of view however more accurate data is required regarding stabilized formation temperatures. For the oil well, the IFTs obtained with the PIC inverse algorithm are close to the true IFTs and compare well with results of simpler methods like the spherical-radial heat flow (Ascencio et al, 1994), the Hasan-Kabir (1994) methods. In general, the simpler analytical methods require at least three temperature measurements to estimate the IFTs whereas the PIC method requires only one temperature log, which represents an advantage from a technical and economic point of view for the geothermal and oil industries. Further applications and validations of the present methods include a wider data set from oil and geothermal wells.

6. REFERENCES

Ascencio, F., García, A., Rivera, J., and Arellano, V.: Estimation of undisturbed formation temperatures under spherical radial heat flow conditions, *Geothermics*, **23(4),** 1994, 317-326.

Dowdle, W.L., and Cobb, W.M.: Static formation temperatures from well logs – an empirical method, *Journal of Petroleum Technology*, (1975), 1326-1330.

Farris, R. F.: A practical evaluation of cement for oil wells. In: *Drilling Production Practice*, American Petroleum Institute, **11**, (1941), 283-292.

Fujino, T., and Yamasaki, T.: The use of fluid inclusion geothermometry as an indicator of reservoir temperature and thermal history in the Hatchobaru geothermal field, Japan. *Geothermal Resources Council Transactions*, **9**, (1985) 429-433.

García-Gutiérrez, A., Espinosa, G., Santoyo, E., Mendoza, P., and Hernández, I.: GEOTRANS: A computer code for estimating transient temperatures in the completion of geothermal wells with drilling losses, *Proceedings*, World Geothermal Congress, Kyushu–Thohoku, Japan, May 28-June 10, (2000), 4023-4028.

Garcia-Gutierrez, A., Ramos-Alcantara, J.R., Iglesias, E.R., and Arellano, V.M.: An inverse method for estimation of for initial temperatures in geothermal reservoirs: Part 1: Mathematical model of the well and formation, *Energy Sources*, (2009), in press.

Grant, M.A., Donaldson, I.G., and Bixley, P.F.: *Geothermal Reservoir Engineering*, Academic Press, New York, (1969).

Hasan, A.R., and Kabir, C.S.: Static reservoir temperature determination from transient data after mud circulation. *SPE Drilling and Completion*, (March 1994), 17-24

Kritikos, W.R., and Kutasov, I. M.: Two-point method for determination of undisturbed reservoir temperature. *SPE Formation Evaluation Journal*, (March 1988), 222-226.

Kutasov, I.M., and Targhi, A.K.: Better deep-hole BHTC estimations possible. *Oil and Gas Journal*, (May1987), 71-73.

Luhesi, M. N.: Estimation of formation temperature from borehole measurements, *Geophysical Journal of the Royal Astronomical Society*, **74, (**1983), 747-776.

Marquardt, W.D.: An algorithm for least squares estimation of non linear parameters. *Journal Society Industrial Appl. Math.*, **11:2**, (1963), 431-441.

Olea-González, U.: *Transferencia de calor en la construcción de pozos petroleros: método inverso*. PhD Thesis, CENIDET, México, (2007), 178 pp.

Olea-Gonzalez, U. and Garcia-Gutierrez A.: Estimation of static formation temperatures in geothermal and oil wells by inversion of logged temperatures, *Geothermal Resources Council Transactions*, **32,** (2008), 53-56.

Osato, K., Ujo, S., and White, S.P.: Prediction of formation equilibrium temperature while drilling based on drilling mud temperature: inverse problem using TOUGH2 and wellbore thermal model. *Proceedings,* TOUGH Symposium 2003, Lawrence Berkeley National Laboratory, Berkeley, CA (2003).

Ramos-Alcantara, J.R.: *Estimación de temperaturas de yacimientos geotérmicos a partir de las temperaturas de entrada y salida de los fluidos de perforación*. MSc Thesis, Centro Nacional de Investigación y Desarrollo Tecnológico, Cuernavaca, México, (2004), 122 pp.

Takahashi, W., Osato, K., Takasugi, S., and White, S.P.: Estimation of formation temperatures from the inlet and outlet mud temperatures while drilling, *Proceedings*, 22nd Workshop on Geothermal Reservoir Engineering, Stanford University, Stanford, CA, (1997), 279-286.

Whitaker, S.: *The Method of Volume Averaging.* Kluwer Academic Pubs., The Netherlands, (1999).